N-ethyl Carbazole-1-Allylidene-Based Push-Pull Dyes as Efficient Light Harvesting Photoinitiators for Sunlight Induced Polymerization

Ke Sun, Shaohui Liu, Hong Chen, Fabrice Morlet-Savary, Bernadette Graff, Corentin Pigot, Malek Nechab, Pu Xiao, Frédéric Dumur, Jacques Lalevée

N-ethyl Carbazole-1-Allylidene-Based Push-Pull Dyes as Efficient Light Harvesting Photoinitiators for Sunlight Induced Polymerization

Ke Sun[1,2], Shaohui Liu[1,2], Hong Chen[1,2], Fabrice Morlet-Savary[1,2], Bernadette Graff[1,2], Corentin Pigot[3], Malek Nechab[3], Pu Xiao[4*], Frédéric Dumur[3*], Jacques Lalevée[1,2*]

[1] Université de Haute-Alsace, CNRS, IS2M UMR 7361, F-68100 Mulhouse, France

[2]Université de Strasbourg, France

[3]Aix Marseille Univ, CNRS, ICR UMR 7273, F-13397 Marseille, France

[4]Research School of Chemistry, Australian National University, Canberra, ACT 2601, Australia.

***Corresponding author:** pu.xiao@anu.edu.au (P. X.); frederic.dumur@univ-amu.fr; jacques.lalevée@uha.fr (J. L.)

Abstract: In this article, the free radical polymerization of acrylates was successfully achieved with a series of twelve push-pull chromophores comprising the *N*-ethyl carbazole-1-allylidene group as the electron-donating group. Using this strong donor, the resulting dyes, never synthesized before, could efficiently initiate the free radical photopolymerization of acrylates upon mild irradiation conditions *e.g.* using a light emitting diode (LED) at 405 nm. These novel multi-component systems comprising the above mentioned push-pull dyes, a tertiary amine (ethyl dimethylaminobenzoate EDB) and an iodonium salt could act as efficient photoinitiating systems (PISs) in free radical polymerization (FRP), leading to the formation of 3D patterns with precise shapes under the direct laser write (DLW) approach. Among these new PISs, dyes 3, 6, 7 and 8 were selected due to their efficient photoinitiation performances for chemical

mechanism studies including steady state photolysis, fluorescence quenching measurements, electron spin resonance (ESR) spin-trapping experiments and cyclic voltammetry. Markedly, their excellent photochemical reactivities prompted us to investigate the performance of these multi-component photoinitiating systems upon sunlight as an ecofriendly approach. As a result, this research proved that sunlight could be used as a potential light source that can advantageously replace LEDs when highly reactive push-pull dyes are used as photosensitizers for the free radical photopolymerization of acrylate resins. Finally, 3D patterns could be prepared with the new photocomposites, and silica fillers could be even incorporated within the photosensitive resins so that a gradient of resolution could be successfully demonstrated.

Keywords: push-pull dye; free radical polymerization; three-component system; LED; sunlight; 3D printing.

Table of contents (TOC):

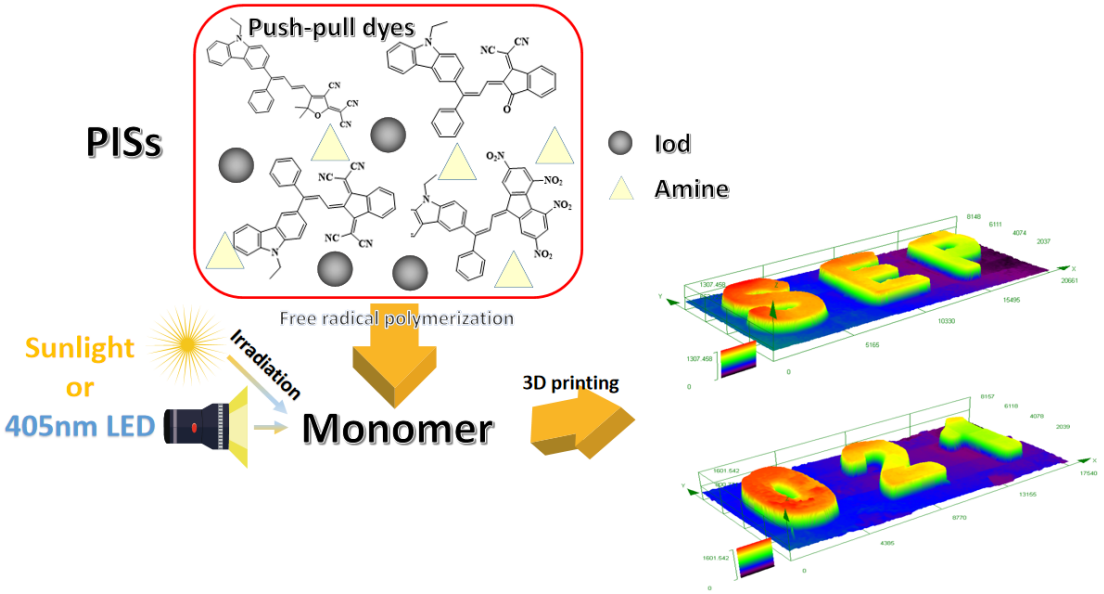

1. Introduction

In recent years, a wide range of push-pull dyes differing by the electron-donating or the electron-accepting groups have been investigated in various applications and reported for their attractive features such as high molar extinction coefficients, strong light absorption in the visible range and the tunability of the absorption spectra.[1-6] In fact, contrarily to numerous dyes for which their absorption spectra are difficult to tune, push-pull dyes have been extensively studied as visible light sensitive photoinitiators of polymerization due to their excellent photoinitiation abilities.[7-11] Indeed, due to the presence of the π-conjugated spacer introduced between the electron donor and the electron acceptor, but also by the possibility to finely tune the electron-donating and electron-accepting abilities of both the donor and the acceptor, position of the intramolecular charge transfer (ICT) band can be carefully controlled.[12] By elongating the length of the π-conjugated spacer, a significant increase of the molar extinction coefficients can also be achieved.[13-15] Benefiting from these different advantages, push-pull dyes have been investigated in a wide range of applications ranging from Organic Electronics, e.g. organic photovoltaics (OPVs),[16,17] organic light-emitting diodes (OLEDs),[18] organic-field effects transistors (OFETs)[19] to nonlinear optics (NLO)[20-26] and waste-water treatment.[27]

Recently, sunlight-induced photopolymerization has attracted the interest of chemists and polymerists, and intense efforts are currently devoted to this research field.[28-31] Using sunlight to initiate a photopolymerization process is attracting increasing attentions due to the numerous advantages. For instance, the emission spectrum of the Sun is relatively broad so that it is well adapted to panchromatic photoinitiators. At least, polymerization reactions can be carried out at room temperature, and the replacement of LEDs by Sunlight can avoid the use of artificial energy.[32] Sunlight is also a free and unlimited light source and constitutes an unlimited resource on Earth. Even if some papers were noticeably devoted to this topic, the reported systems don't exhibit very high reactivity.[33-35] Indeed, Free radical polymerization under sunlight still remains a challenge due to the low light intensity

requiring extremely efficient systems. Moreover, preparation of polymer composites containing fillers is another active research field so that the combination of the two topics and the development of new photoinitiating systems that could both address the polymerization under sunlight and the polymerization of resins containing fillers could constitute a major breakthrough in photopolymerization.

Here, in this article, a new series of push-pull dyes, never reported before, (Figure 1) and containing the *N*-ethyl carbazole-1-allylidene moiety as the electron-donating group have been used as photoinitiators with co-initiators, i.e. an iodonium salt and a tertiary amine (ethyl dimethylaminobenzoate EDB), to initiate the FRP of a benchmark acrylate monomer, TA. As a result, three-component photoinitiating systems comprising dyes 3, 6, 7, 8 furnished high final acrylate function conversions. Photopolymerization processes were monitored by Real-Time Fourier Transform Infrared spectroscopy (RT-FTIR), and the new photoinitiating systems were successfully applied to the elaboration of 3D patterns with excellent spatial resolutions by the direct laser write (DLW) approach. Photopolymerization was also successfully induced by sunlight in short photo-activation times and it proved to be an efficient approach to replace the energy-consuming LEDs. The photochemical properties and the chemical mechanisms of the selected push-pull dyes were investigated by photolysis and fluorescence measurements. The use of electron spin resonance (ESR) spin-trapping technique further confirmed the proposed mechanisms. Finally, 3D patterns obtained with silica-containing composites demonstrated the usability of the novel push-pull dyes in practical composites applications.

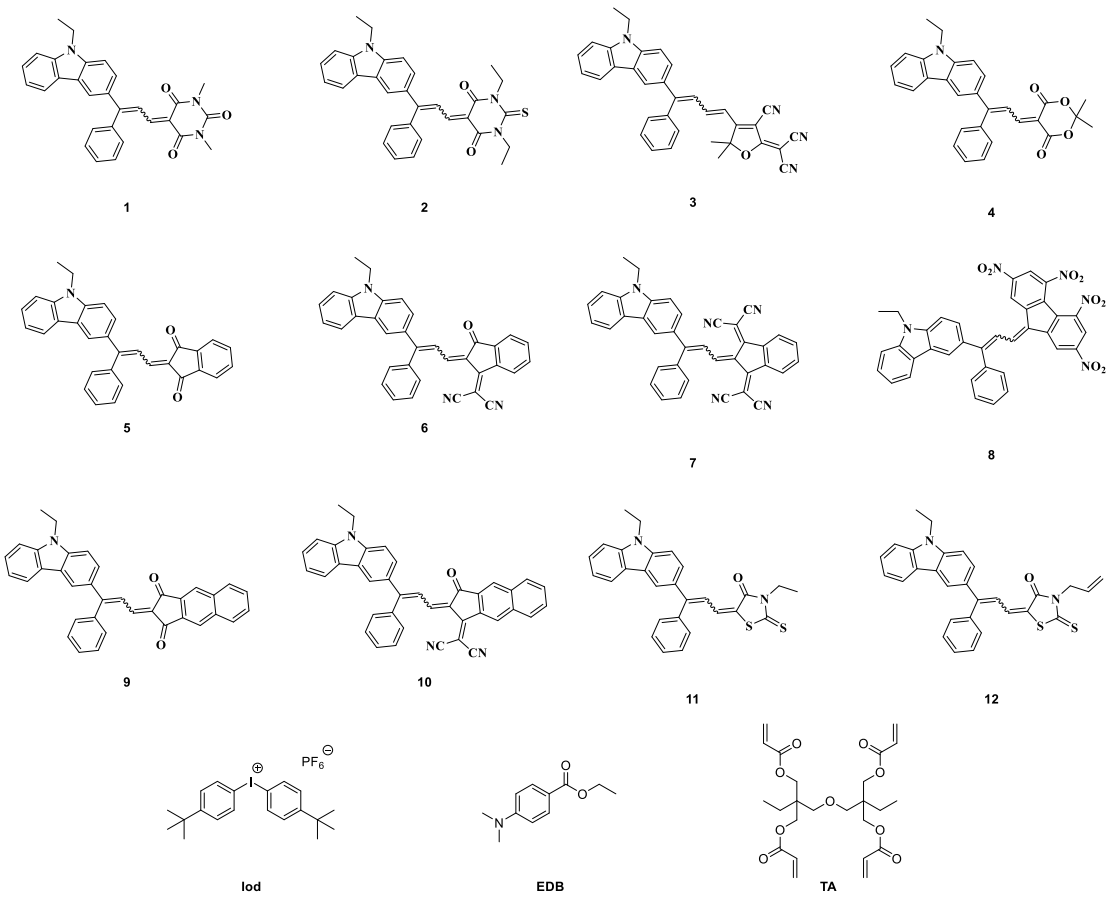

Figure 1. Chemical structures of dye **1-12**, iodonium salt (Iod), the amine (EDB) and the acrylate monomer (TA) used in this study.

2. Materials and Methods

2.1. Dyes

Molecular structures of investigated dyes 1-12 based on a push-pull structure in this article are depicted in the Figure 1. The synthesis procedures are reported in Section 3.1 and their characterization reported in supporting information.

2.2. Other Materials

A commercial iodonium salt (Iod - Speedcure 938) and an amine (ethyl

dimethylaminobenzoate - EDB) were used as co-initiators in this article. Their corresponding chemical structures are given in Scheme 1. These different chemicals were purchased from Lambson Ltd (UK). The benchmark acrylate monomer (TA) was purchased from Allnex and its corresponding chemical structure is also shown in Figure 1. All photopolymerization processes reported in this work were performed in mild conditions e.g. solvent-free and mild light irradiation conditions at room-temperature to develop green synthetic approaches towards polymers.

2.3. Polymerization profiles obtained by Real Time Fourier Transformed Infrared Spectroscopy (RT-FTIR)

The novel three-component photoinitiating systems were prepared by mixing the dyes, the iodonium salt (Iod) and the amine (EDB) as weight content ratios: 0.1%/2%/2% w/w/w in a benchmark monomer (tetrafunctional polyether acrylate noted TA), respectively. 2 Drops of prepared photosensitive formulations were deposited in laminate between 2 polypropylene films, then exposed to irradiation upon LED emitting at 405 nm (I_0 = 110 mW.cm^{-2}) at room temperature and under air for the Free Radical Polymerization (FRP); the thickness was controlled ~ 100 μm. The vibration peak of the acrylate functionality was continuously monitored at ~6130 cm^{-1} by real-time FTIR spectroscopy (JASCO FTIR 4100) to follow the polymerization kinetics. The polymerization profiles were established using the following relationship of conversion and irradiation time:[36-39]

$$\text{conversion (\%)} = (A_0 - A_t)/A_0 \times 100 \qquad \text{(eq 1)}$$

where A_0 is the initial peak area before irradiation and A_t is the peak area after irradiation for a given time t.

2.4. The chemical mechanisms studied by steady state UV-Visible absorption photolysis and Fluorescence spectroscopy

Chemical mechanisms involved in the three-component PISs were investigated by combining several techniques, namely UV-visible absorption spectroscopy (JASCO V730 UV–visible spectrometer) used to record the UV-visible absorption spectra in photolysis experiments and a JASCO FP-6200 spectrofluorimeter for the fluorescence properties. The Stern-Volmer coefficients (Ksv) were calculated by the slopes of Stern−Volmer treatment for fluorescence quenching and the electron transfer quantum yields (ϕ_{et}) were determined using the eq. 2:[37, 38]

$$\phi_{et} = K_{sv}[\text{additive}]/(1+K_{sv}[\text{additive}]) \quad \text{(eq 2)}$$

2.5. Cyclic voltammetry

The redox potentials of all dyes (oxidation potential noted E_{ox} and reduction potential noted E_{red}) were determined as follow. The dyes were dissolved in acetonitrile while using tetrabutylammonium hexafluorophosphate as the supporting electrolyte (potential vs. Saturated Calomel Electrode, SCE). The singlet excited state energy level (Es_1) was calculated from the crossing point of the UV-visible and fluorescence spectra. Thus, the free energy change from the singlet state (ΔG^{S1}_{Iod} or ΔG^{S1}_{EDB}) for the electron transfer reaction was determined with E_{ox}, E_{red}, and Es_1 which were calculated from equations 3 and 4.[40] Similarly, the free energy change from the triplet state (ΔG_{et}) was calculated with E_{ox}, E_{red}, and E_{T1} from equations 5 and 6[40] whereas the triplet state energy level (E_{T1}) was extracted from molecular energy level calculations (Gaussian 03 suite of programs). The reduction potential used for the iodonium salt was of -0.7 V[41] and the oxidation potential of EDB was of 1.0 V according to the literature data.[42]

$$\Delta G^{S1}_{Iod} = E_{ox} - (-0.7) - E_{S1} \quad \text{(eq 3)}$$

$$\Delta G^{S1}_{EDB} = 1 - (E_{red}) - E_{S1} \quad \text{(eq 4)}$$

$$\Delta G^{T1}_{Iod} = E_{ox} - (-0.7) - E_{T1} \quad \text{(eq 5)}$$

$$\Delta G^{T1}_{EDB} = 1 - (E_{red}) - E_{T1} \quad \text{(eq 6)}$$

2.6. Photocomposites preparation

Photocomposites were prepared with three-component systems (dye/Iod/EDB, 0.1w%/2%/2%, w/w/w/) and a weight content of 20% was used for the silica fillers dispersed in the monomer (TA).

2.7. 3D printing experiments

Photosensitive formulations (TA as monomer) including PISs or PISs/silica was dropped onto a 2 mm-thick homemade tank and polymerized upon irradiation with a computer-controlled laser diode @405 nm with spot size around 50 μm. By direct laser write (DLW), tridimensional patterns of precise shapes could be prepared. Following their fabrications, the different 3D patterns were characterized by a numerical optical microscope (DSX-HRSU, OLYMPUS corporation).[43, 44]

2.8. Electron Spin Resonance (ESR) Spin Trapping (ESR-ST)

Radicals formed during polymerization could be observed by Electron Spin Resonance (Spin Trapping) experiments using an X-band spectrometer (Bruker EMXplus), enabling to confirm the proposed chemical mechanisms. The solutions (dye/Iod or dye/EDB in *tert*-butylbenzene) were treated under a nitrogen saturated atmosphere at room temperature before irradiation. *N*-*tert*-Butyl-phenylnitrone (PBN) was used as the spin trap agent. ESR spectra simulations were carried out using PEST WINSIM software.[37, 38]

2.9. Computational procedure

Geometry optimizations were performed at the UB3LYP/6-31G* level. Geometries were frequency checked and the molecular orbitals (MOs) involved in these transitions were extracted. The triplet state energy levels were calculated at this DFT level.[45, 46]

3. Results and Discussions

3.1. Synthesis of the different dyes

The extended aldehyde **Cbz-BP** has synthesized in three steps starting from 9-ethyl-9*H*-carbazole. Especially, **Cbz-BP** was prepared by following a procedure previously used to convert Michler's ketone to Michler's aldehyde.[47] Notably, by performing a Friedel-Craft reaction on 9-ethyl-9*H*-carbazole with benzoyl chloride in the presence of aluminum chloride, (9-ethyl-9*H*-carbazol-3-yl)(phenyl)methanone could be prepared in 84% yield. Reduction with methylmagnesium iodide furnished 9-ethyl-3-(1-phenylvinyl)-9*H*-carbazole in almost quantitative yield (See Scheme 1). Formylation of the alkene by a Vilsmeier Haack reaction gave **Cbz-BP** as a mixture of s-cis/s-trans isomers that could not be separated by column chromatography. If no structural determination was carried out to identify which isomer was the main product, a 2:1 ratio could be found on the proton NMR spectrum of **Cbz-BP**. This mixture of isomers was subsequently used for the synthesis of the different dyes.

The different dyes of the series were prepared by a Knoevenagel reaction done in basic conditions. Except for dye **7** for which diisopropylamine (DIPEA) was used instead of piperidine, all dyes could be obtained with reaction yields ranging from 82 to 92% (see Scheme 2). In the case of dye **6**, choice of DIPEA as the base was motivated by recent results reported in the literature mentioning a nucleophilic attack of secondary amines on the cyano groups of **EA6**, inducing a cyclization reaction and producing azafluorenone derivatives.[12, 48-51] Finally, dye **7** had to be prepared by using a specific procedure. Indeed, due to the remarkable stability of the **EA7** anion in basic conditions,

no condensation reaction can occur with an aldehyde. To circumvent this problem, the condensation of **Cbz-BP** and **EA7** in acetic anhydride furnished dye **7** in 85% yield.

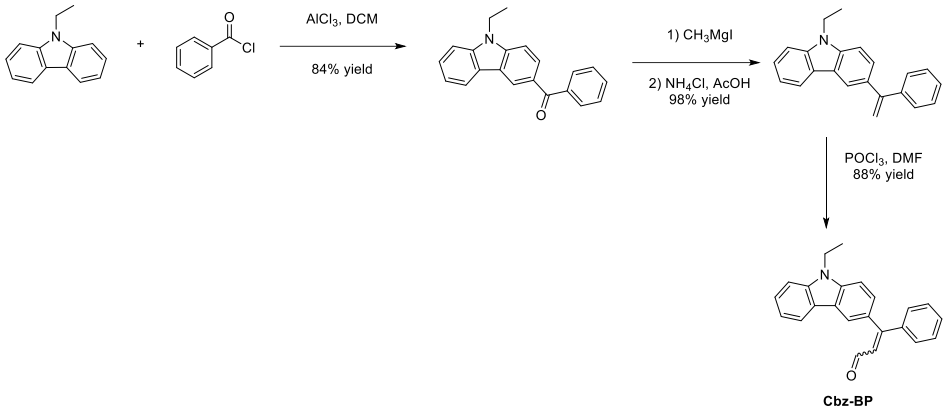

Scheme 1. Synthetic route to **Cbz-BP**.

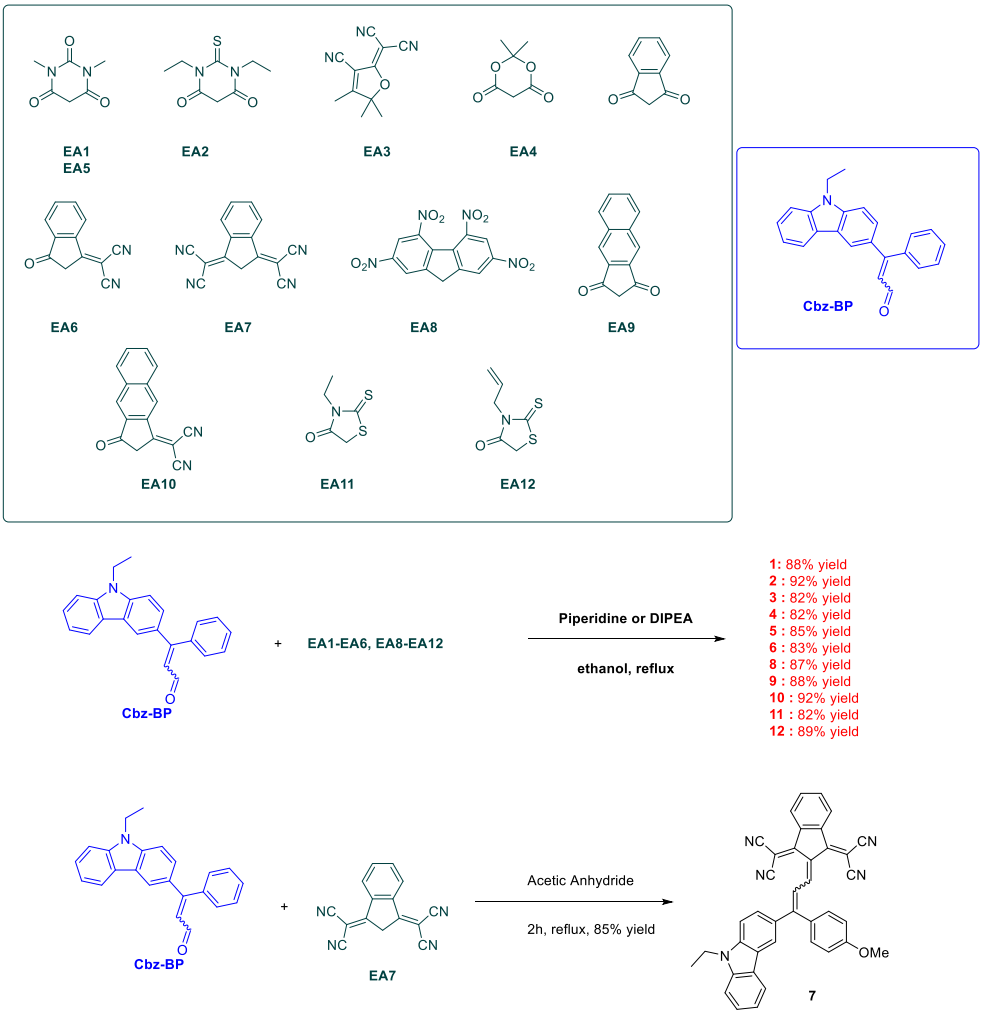

Scheme 2. Synthetic route to dyes **1-12**.

In the case of symmetric electron acceptors (**EA1**, **EA2**, **EA4**, **EA5**, **EA7**, **EA8** and **EA9**), the corresponding dyes (**1**, **2**, **4, 5** and **7-9**) were obtained as a mixture of *s*-cis and *s*-trans isomers. Conversely, a more complex situation was found for dyes prepared with **EA3**, **EA6**, **EA10**, **EA11** and **EA12**, since in complement of a *s*-cis/*s*-trans mixture, the different electron acceptors could adopt two different orientations so that a mixture of 4 isomers could be theoretically obtained in these cases (See Figure 2). Besides, the steric hindrance induced by the use of asymmetric electron acceptors such as **EA6** and **EA10** certainly favour an orientation over the others. It has to be noticed that among the twelve electron acceptors used in this study, **EA3**[52], **EA6**[53], **EA7**[54], **EA8**[55], **EA9**[56] and **EA10**[48] had to be prepared.

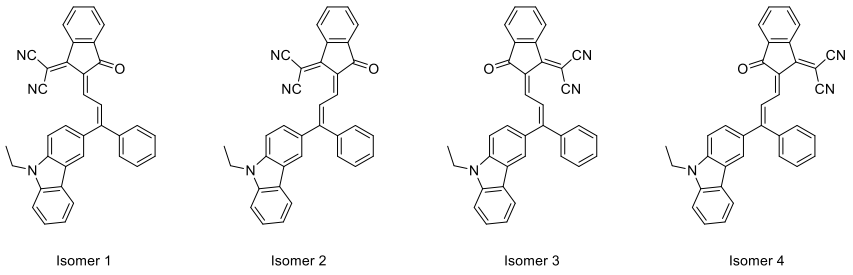

Figure 2. The four possible isomers when asymmetric electron acceptors are used.

3.2 Photopolymerization kinetics with the newly proposed push-pull dyes in three-component photoinitiating systems

As depicted in Figure 3a, photopolymerization kinetics of TA upon irradiation with a LED at 405 nm using three-component photoinitiating systems (PISs) composed of the different dyes (from dye 1 to 12, 0.1% in monomer, w/w), the iodonium salt (used as electron acceptor, 2% in monomer, w/w) and the amine (used as electron donor, 2% in monomer, w/w) were monitored by Real-Time Fourier Transform Infrared spectroscopy (RT-FTIR) at room temperature. As observed for dyes 1-12, the final acrylate function conversions (FCs) determined at 400 s are gathered in the Table 1 as well as the monomer conversions obtained with the reference two-component PIS (2% Iod: 2% amine in TA) without dyes (cited as dye 0/blank in Table 1). In fact, based on

their photoinitiating abilities, the series of twelve dyes can be divided into two different families:

(1) those exhibiting a good photoinitiating ability such as dyes 3, 6, 7, 8 with high final conversions (FCs) reaching 98% or above. Polymerizations carried out with these dyes were also characterized by short induction period ($T-T_0$ with T: Start time of polymerization; T_0: Start time of light irradiation). Typically, polymerization processes are ended within 50s, evidencing their remarkable photoinitiation abilities. In this latter series, the dye 7 is found the best one (combining high polymerization rate, low inhibition time and high FC).

(2) All the other dyes showed less efficiency and lower FCs comparing with the reference two-component PISs without dye. Their FCs obtained with these dyes only furnished 96% conversions or below. Interestingly, the lowest acrylate function conversion was obtained with dye 2, which only reached 83% after 400 s of irradiation at 405 nm.

In light of the good photoinitiating abilities of dyes 3, 6, 7 and 8, the first family composed of these four push-pull dyes was thus selected for further investigations concerning the light absorption properties of photoinitiators and the chemical mechanisms examined in the following parts. Additionally, an order of induction time could be established with the four most reactive dyes examined in this work, namely dye 7 > dye 6 > dye 3 > dye 8.

To investigate the photoinitiation abilities more precisely and comprehensively, the photopolymerization profiles of TA initiated by dye 7 or dye 8-based PIS upon sunlight irradiation were also established and these latter are shown in Figure 3b (for dye 8) and Figure 3c (for dye 7). Remarkably, dye 7 and 8 acted as an excellent photoinitiator with high performance and furnished high final reactive function conversions (~99%) for the polymerization of TA under sunlight. Thus, photoinitiated processes done under mild conditions such as irradiation with sunlight provide novel

solutions in the field of FRP, especially, the possibility to polymerize without using energy.

Furthermore, the polymerization of TA can also be observed under irradiation of LED or sunlight using one-component PIS, which only dye 7 (or dye 8) included without iodonium salts or amine. The photopolymerization kinetics are shown in Figure 3b or 3c (under 405nm LED for black curve, sunlight for red curve, respectively). Remarkably, all these data indicate that dye 7 (or 8) can be used as an efficient photoinitiator in photopolymerization, and sunlight was efficient as a reliable light source to initiate polymerization. This is ascribed to the panchromatic behavior of dyes 7 and 8 as light harvesting compounds (see in Figure S1 their broad absorption properties on the 350-700 nm range).

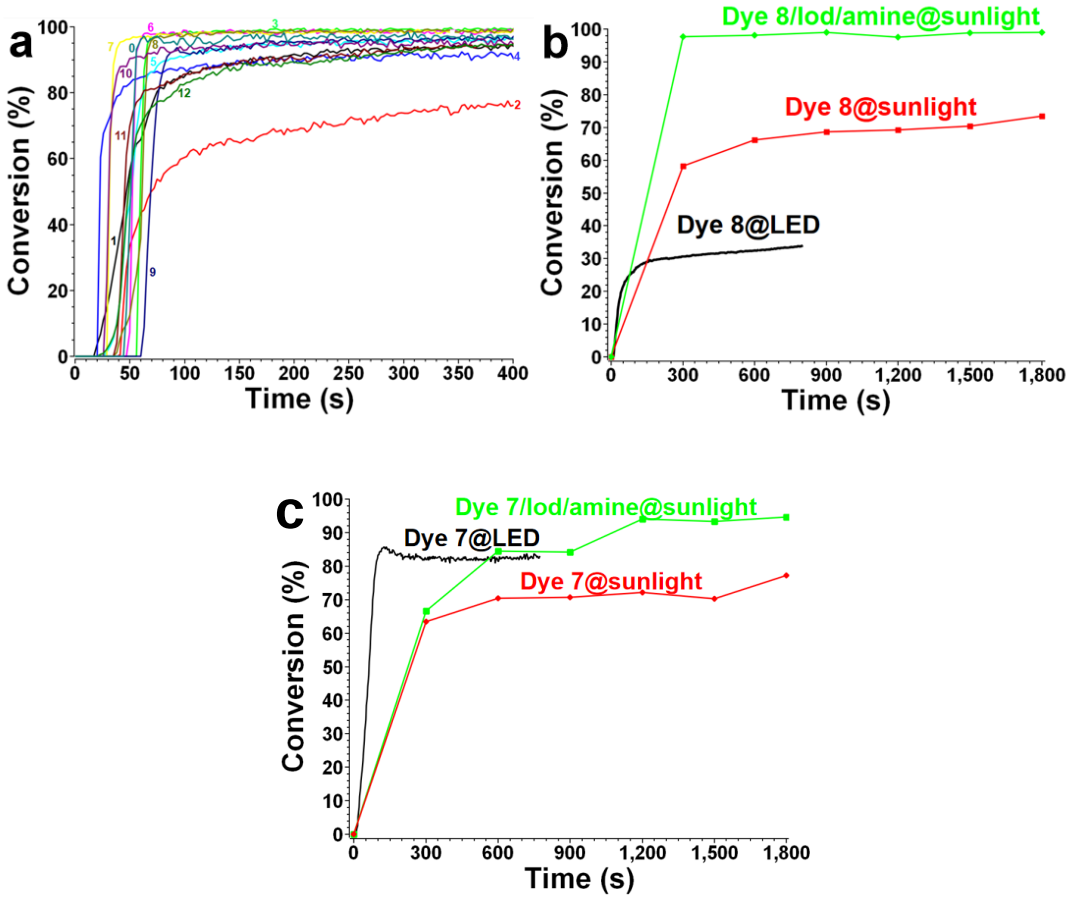

Figure 3. **(a)** Photopolymerization profiles of TA (conversion of C=C bonds vs irradiation time) initiated by iodonium salts and EDB upon exposure to LED@405nm in laminate in the presence of dyes 1-12 at the same weight ratio: dye:Iod:EDB = 0.1%:2%:2% in TA. Curve 0: Iodonium salt: EDB=2%:2% in TA without dye; **(b)**

Photopolymerization profiles of TA (conversion of C=C bonds vs irradiation time) initiated by: **(green)** the iodonium salt and EDB upon exposure to sunlight in laminate in the presence of dye 8 at the weight ratio: dye:Iod:EDB=0.1%:2%:2% in TA. **(red)** dye 8 (weight ratio: 0.1% in TA) alone upon exposure to sunlight in laminate. **(black)** dye 8 (weight ratio: 0.1% in TA) alone upon exposure to LED@405nm in laminate. **(c)** Photopolymerization profiles of TA (conversion of C=C bonds vs irradiation time) initiated by: **(green)** the iodonium salt and EDB upon exposure to sunlight in laminate in the presence of dye 7 at the weight ratio: dye:Iod:EDB=0.1%:2%:2% in TA. **(red)** dye 7 (weight ratio: 0.1% in TA) alone upon exposure to sunlight in laminate. **(black)** dye 7 (weight ratio: 0.1% in TA) alone upon exposure to LED@405nm in laminate.

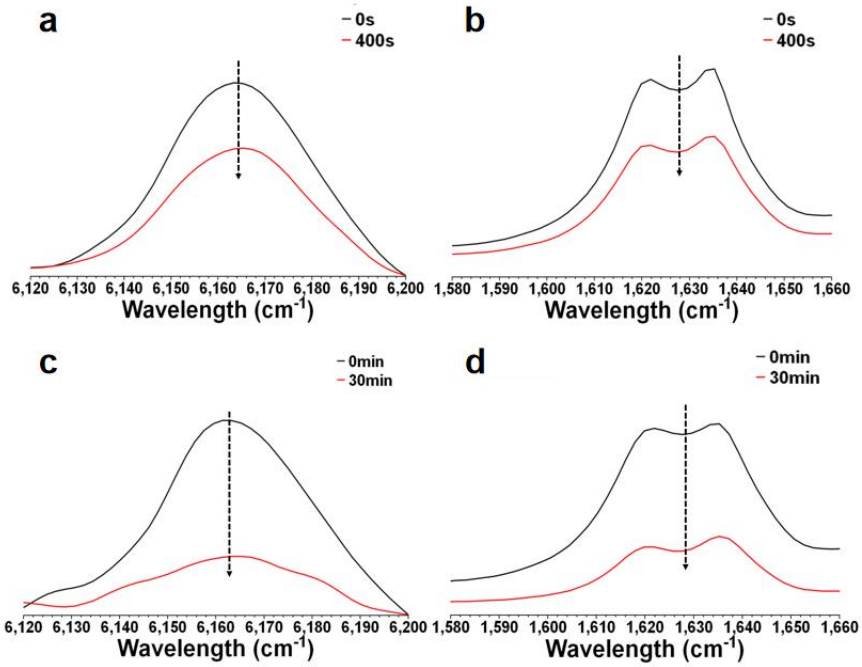

Figure 4. FT-IR spectra of before and after the photopolymerization of monomer TA initiated by dye 8 alone (weight ratio: 0.1% in TA) in laminate: **(a)** upon exposure to LED@405nm LED for the acrylate functional peak ranging from 6120cm^{-1} to 6200cm^{-1}; **(b)** upon exposure to LED@405nm for the acrylate functional peak ranging from 1600cm^{-1} to 1660cm^{-1}; **(c)** upon exposure to sunlight for the acrylate functional peak ranging from 6120cm^{-1} to 6200cm^{-1}; **(d)** upon exposure to sunlight for the acrylate functional peak ranging from 1600cm^{-1} to 1660cm^{-1}.

Table 1. Summary of the final acrylate function conversions (FCs) at 405 nm (dye 8 at sunlight included) for TA using three-component photoinitiating systems: dyes (0.1%, w/w), iodonium salt (2%, w/w) and amine (2%, w/w). The final function conversion of two-component photoinitiating system without dye (Iod/amine) was cited as blank.

Dye	Blank	1	2	3	4	5	6

FCs	97%	95%	83%	99%	91%	96%	98%
Dye	**7**	**8**	**8 (sunlight)**	**9**	**10**	**11**	**12**
FCs	98%	99%	99%	96%	95%	96%	96%

3.3. Direct laser write (DLW) experiments

Following the examination of the photoinitiating abilities of the different dyes, the polymerization of TA acrylate in DLW experiments was examined and initiated with a selected set of three-component systems (dye 3 (or 6, 7, 8)/Iod/amine). These systems were selected due to their excellent behaviors in FRP. The formation of tridimensional patterns ("SY" for dye 3, "SK" for dye 6, "RZ" for dye 7, "ZH" for dye 8) was successfully observed in a very short time and specificities of these 3D profiles, e.g. smooth surfaces, excellent spatial resolution, were demonstrated by profilometric observations via numerical optical microscopy (see Figure 5).

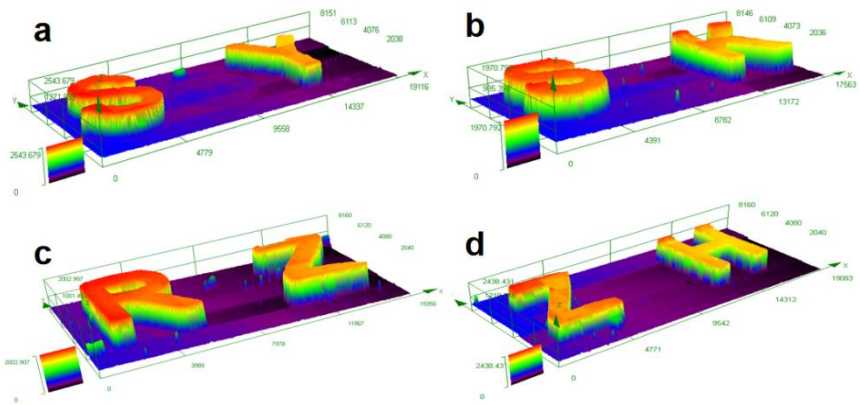

Figure 5. Free radical photopolymerization experiments in DLW experiments initiated by dye-based three-component photoinitiating systems in TA. Characterization of 3D patterns overall appearance: color patterns observed by numerical optical microscopy in the presence of: **(a)** dye 3/Iod/EDB (0.1%/2%/2% w/w/w); **(c)** dye 6/Iod/EDB (0.1%/2%/2% w/w/w). **(b)** dye 7/Iod/EDB (0.1%/2%/2% w/w/w); **(d)** dye 8/Iod/EDB (0.1%/2%/2% w/w/w).

3.4. Photochemical properties of dyes 3, 6, 7 and 8

3.4.1. Light absorption properties of the push-pull dyes

Molar extinction coefficients of dyes were determined by UV-visible absorption spectroscopy in acetonitrile (see Figure S1) and the light absorption parameters are gathered in Table 2. As shown in Figure S1, the high maximum molar extinction coefficients at the maximum absorption wavelengths (λ_{max}) are ranging between 6440 $M^{-1}.cm^{-1}$ for dye 9 and 53200 $M^{-1}.cm^{-1}$ for dye 12, from 454 nm for dye 11 to 579 nm for dye 10, respectively (see Table 2). For more details, dyes 3, 5, 11, 12 showed very high maximum molar extinction coefficients which were higher than 40 000 $M^{-1}.cm^{-1}$ at their maximum absorption wavelengths (λ_{max}) e.g. ε(Dye 3) = 42 460 $M^{-1}.cm^{-1}$ at λ_{max} = 531 nm, ε(Dye 5) = 43 480 $M^{-1}.cm^{-1}$ at λ_{max}= 479 nm. ε(Dye 11) = 41 120 $M^{-1}.cm^{-1}$ at λ_{max} = 454 nm, ε(Dye 12) = 53 200 $M^{-1}.cm^{-1}$ at λ_{max} = 456 nm, in the UV-visible absorption range. Interestingly, compared to dyes 1, 2, 11, 12, dyes 3, 6, 7 showed relatively poor extinction coefficients at 405 nm: 11 150 $M^{-1}.cm^{-1}$ for dye 3, 8430 $M^{-1}.cm^{-1}$ for dye 6 and 7000 $M^{-1}.cm^{-1}$ for dye 7 which not fit to their photoinitiation abilities and which was discussed in the section of 3.2. Parallel to this, dyes 4, 9, 10 which showed lower molar extinction coefficients (less than 30 000 $M^{-1}.cm^{-1}$) at their absorption maxima also proved to be poorer photoinitiators, even if higher molar extinction coefficients were detected at 405 nm for dyes 4 and 10 (reaching 10 000 $M^{-1}.cm^{-1}$) compared to that of dyes 6, 7. In the case of dye 8, both good photoinitiation abilities and high molar extinction coefficients (ε_{max} = 33500 $M^{-1}.cm^{-1}$ at λ_{max} = 447 nm, $\varepsilon_{@405nm}$= 19500 $M^{-1}.cm^{-1}$) were found for this dye, and the results confirmed the high performances of dye 8 as a reactive photoinitiator in free radical polymerization under exposure to both 405 nm LED and sunlight.

Table 2. Light absorption properties of the different push-pull dyes in acetonitrile: maximum absorption wavelengths λ_{max}; extinction coefficients at λ_{max} (ε_{max}) and

extinction coefficients at the emission wavelength of the LED@405 nm($\varepsilon_{@405nm}$).

	λ_{max} (nm)	ε_{max} ($M^{-1}.cm^{-1}$)	$\varepsilon_{@405nm}$ ($M^{-1}.cm^{-1}$)
Dye 1	465	38560	18230
Dye 2	502	37700	13800
Dye 3	531	42460	11150
Dye 4	460	21280	10600
Dye 5	479	43480	11460
Dye 6	548	32610	8430
Dye 7	548	30030	7010
Dye 8	564	33500	19470
Dye 9	441	6440	4930
Dye 10	579	27610	10860
Dye 11	454	41120	20810
Dye 12	456	53200	26290

3.4.2 Steady state photolysis experiments of dye-based Photoinitiating Systems.

The photolysis process revealed efficient interactions of the dye/Iod or dye/EDB two-component systems. In this part, the chemical mechanisms were confirmed by comparisons between the consumption of dyes in three-component systems dye/Iod/EDB and two-component systems dye/Iod or dye/EDB during photolysis. Furthermore, the weight concentration ratio of dyes/Iod/EDB in acetonitrile are fixed

in all systems and set as: 0.0005%: 2%: 2% in dyes/Iod/EDB systems, 0.0005%: 2% in dyes/Iod systems and 0.0005%: 2% in dyes/EDB systems. Here, we proposed two partial interactions both existing in three-component systems: (1) dye/Iod and (2) dye/EDB. Remarkably, examination of these two reactions in solution was highly representative of the interactions existing in three-component systems.

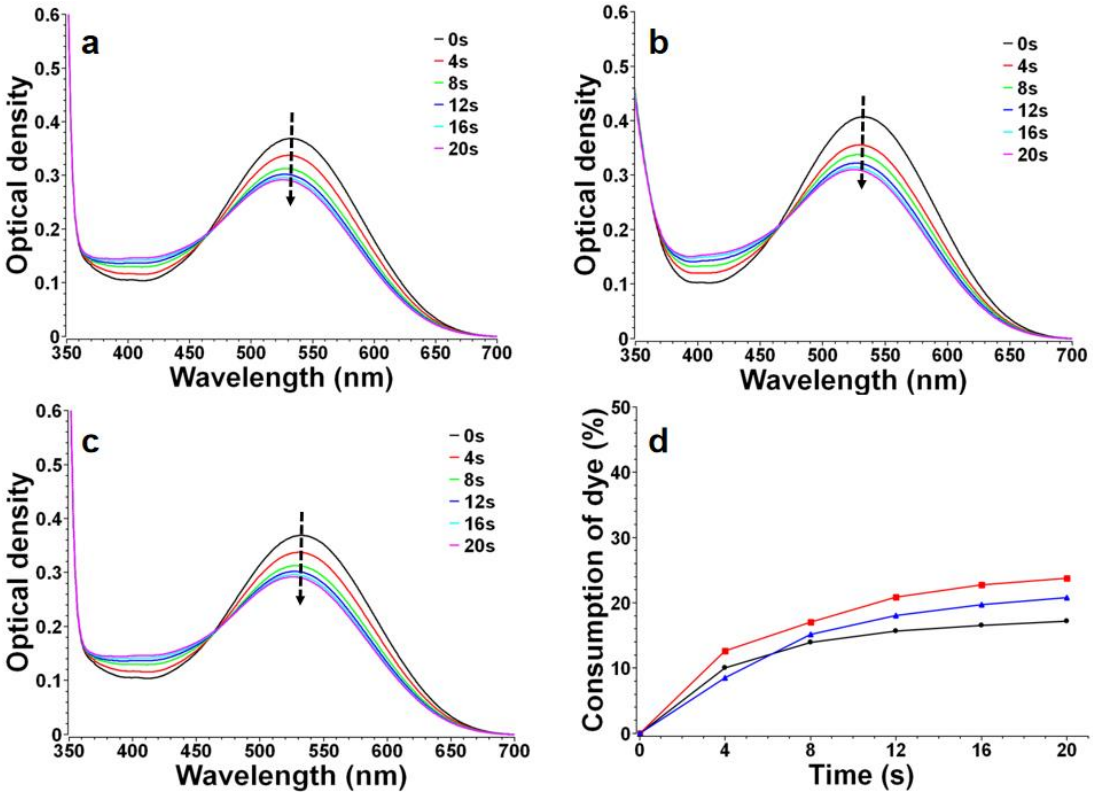

Figure 6. UV-visible absorption spectra of dye 3 (7.77×10^{-6}M) with co-initiators: **(a)** Iod (2.93×10^{-2} M) and EDB (8.15×10^{-2} M), **(b)** Iod (2.93×10^{-2} M) and **(c)** EDB (8.15×10^{-2} M) upon exposure to LED@405nm under air, in acetonitrile. **(d)** Consumption of dye 3 vs. irradiation time @ λ = 405 nm: dye 3/Iod/EDB(●); dye 3/Iod(■); dye 3/ EDB(▲).

As shown in Figure 6, absorption of dye 3 significantly decreased when the Iodonium salt or the amine was used as co-initiators in three-component systems and irradiated at 405 nm with a LED. The percentages of consumption of dye 3 in the three systems: dye/Iod/EDB, dye/Iod, dye/EDB are shown in Figure 6d. These curves can be used as a powerful tool to investigate the chemical mechanisms occurring during

photopolymerization. The chemical interaction between dye 3 and Iod is slightly stronger than dye 3 and amine, which significantly contributed to the integrated reaction of three-component systems.

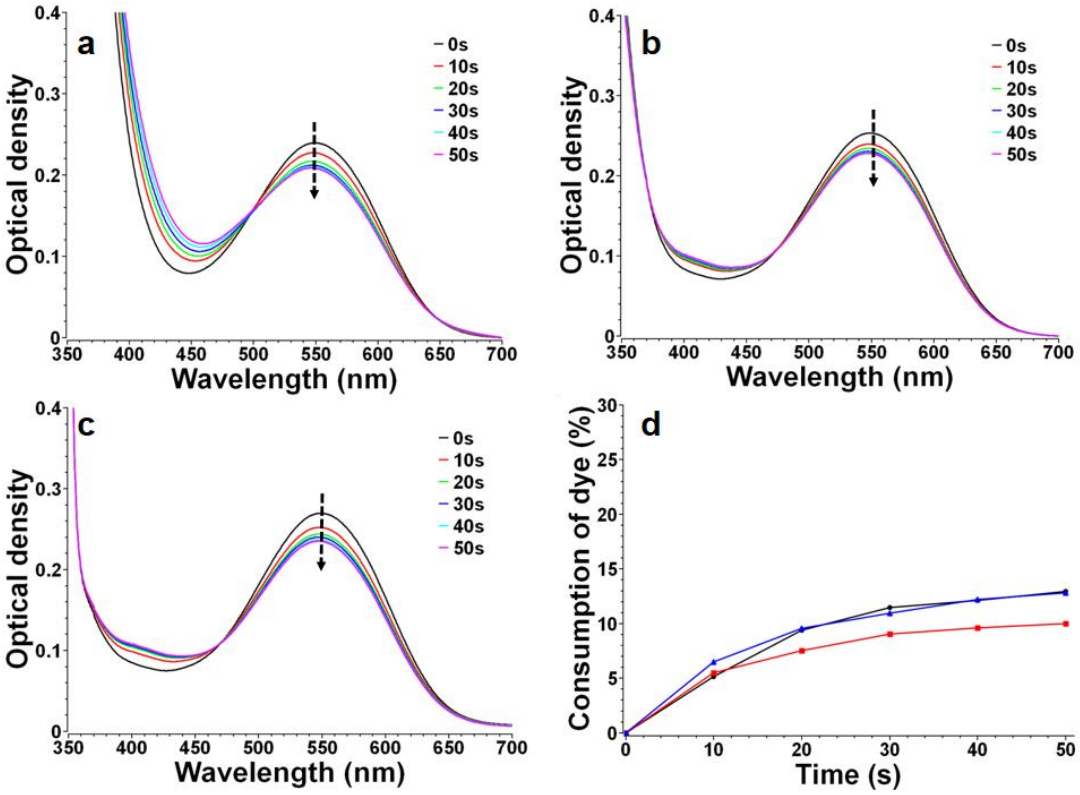

Figure 7. UV-visible absorption spectra of dye 6 (7.85×10^{-6} M) with co-initiators: **(a)** Iod (2.93×10^{-2} M) and EDB (8.15×10^{-2} M), **(b)** Iod (2.93×10^{-2}M) and **(c)** EDB (8.15×10^{-2} M) upon exposure to LED@405nm under air in acetonitrile. **(d)** Consumption of dye 6 vs. irradiation time @ λ = 405 nm: dye 6/Iod/EDB(●); dye 6/Iod(■); dye 6/EDB(▲).

Conversely, dye 6 showed distinct photolysis processes compared to dye 3. Even if the decreasing tendencies were observed during the photolysis of the three systems: dye 6/Iod/EDB, dye 6/Iod and dye 6/EDB, however, photolysis of the dye 6/Iod system seemed to be less efficient than that of dye 6/EDB system: the consumption of dye 6 in dye/Iod only achieved ~10% while the consumption in dye/EDB reached ~13%. A similar process was found in the case of the dye 6/Iod/EDB three-component system

(see Figure 7d), when compared to the dye 6/EDB interaction, indicating that the dye 6/EDB interaction drastically affects the efficiency of the integrated reaction in free radical polymerization process (See Figure 7).

Upon irradiation at 405 nm with a LED, just like for dye 3 and dye 6, photolysis processes were also examined in the case of dye 7-based PISs, comprising the dye 7/Iod/EDB three-component system and the dye 7/Iod or dye 7/EDB two-component systems (see Figure S2a, b, c) upon exposure to the LED. The changes of consumption of dyes in PISs are shown in Figure S2d. Interestingly, it has been demonstrated that dye 7/Iod and dye 7/EDB two-component PISs achieved similar dye-consumption percentages, more precisely, final dye-consumption of dye 7/Iod (~10.5%) was slightly higher than that of the dye 7/EDB system (~9.5%) during the photolysis process, which is different from the behaviors detected during the photolysis experiments of dyes 3 and 6. The consumption of dye 7 can be maximized in PISs composed of the three components (reached ~20%), proving that the interactions between dye 7/Iod/EDB are much efficient than that in the dye 7/Iod or dye 7/EDB two-component systems.

Photolysis experiments were also performed with dye 8-based PISs, still under irradiation with a 405 nm LED. As observed for the previous systems, the three systems (dye 8/Iod/EDB, dye 8/Iod and dye 8/EDB) demonstrated obvious decreasing tendencies as shown in Figure S3. After irradiation, both the final consumptions of dye in two-component systems (dye/Iod and dye/EDB) reached the same value of 11% consumption and 26% consumption for the dye/Iod/EDB system (see Figure S4), indicating that the interactions in three-component systems are comparable to that observed for the dye 7-base PISs.

Parallel to the LED-activated photolysis done with the three-component dye 8/Iod/EDB system, substitution of the 405 nm LED by sunlight to perform the different photolysis experiments was also investigated. As shown in Figure S3b, sunlight significantly activates the photolysis process. Surprisingly, the consumption of dye 8 is significantly accelerated in the presence of sunlight, and a higher dye consumption was

obtained with sunlight than with a 405 nm LED, indicating the possible participation of UV sunlight (see Figure S4).

3.4.3. Potential mechanisms deduced from photolysis reactions.

The chemical mechanisms involved in the three-component photoinitiation systems was established on the basis of the previous experiments. The dye excited states are enabled to be consumed by the EDB/Iod combination and generate radicals: $Dye^{\bullet+}$, $Dye\text{-}H^{\bullet}$, in two pathways of oxidation or reduction reactions as r2, r3 proposed in Scheme 3. After that, the oxidized form $Dye^{\bullet+}$ can be reduced by EDB, regenerating the Dye in its initial state according to the equation r3 in Scheme 3. Similarly, the reduced form $Dye\text{-}H^{\bullet}$ can be oxidized by Iod to finish the catalytic cycle and the original dye was regenerated in the resin. Particularly, the byproducts $Ar^{\bullet}$, $EDB^{\bullet}_{(-H)}$ which are also created in these reaction pathways (see r4, r5 in Scheme 3), can be advantageously used as radicals confirming the chemical mechanisms. Notably, these two species were detected by ESR-spin trapping experiments (see below). The results will be detailed in the next parts of this paper.

(r1) $Dye \rightarrow {}^{*}Dye \qquad (h\nu)$

(r2) $^{*}Dye + Ar_2I^{+} \rightarrow Dye^{\bullet+} + Ar_2I^{\bullet} \rightarrow Dye^{\bullet+} + Ar^{\bullet} + ArI$

(r3) $^{*}Dye + EDB \rightarrow Dye^{\bullet-} + EDB^{\bullet+} \rightarrow Dye\text{-}H^{\bullet} + EDB^{\bullet}_{(-H)}$

(r4) $Dye^{\bullet+} + EDB \rightarrow Dye + EDB^{\bullet+}$

(r5) $Dye\text{-}H^{\bullet} + Ar_2I^{+} \rightarrow Dye + Ar^{\bullet} + ArI + H^{+}$

Scheme 3. Proposed photoinitiation step mechanisms of the dyes/Iod/EDB redox combination.

3.4.4. Chemical mechanisms in electron transfer reactions for dyes

In addition to the aforementioned conclusions, we also determined the theoretical parameters in the electron transfer reaction e.g. the singlet excited state energy (E_{S1}), the free energy changes (ΔG), the triplet state energies (calculated at the density functional theory level), Stern-Volmer coefficients and the electron transfer quantum yields for the investigated dyes, which contributed to get a deeper insight into the chemical mechanisms of FRPs. The different paramaters are listed in the Table 3.

Table 3. Parameters characterizing the electron transfer reactions for the dyes 3, 6, 7, 8 in acetonitrile[a]

	E_{S1} (eV)	E_{T1} (eV)[b]	E_{red} (eV)	E_{ox} (eV)	ΔG^{S1}_{Iod} (eV)	ΔG^{S1}_{EDB} (eV)
Dye 3	1.97	1.26	-0.62	0.29	-0.98	-0.35
Dye 6	2.00	1.45	-0.60	0.18	-1.12	-0.4
Dye 7	2.01	1.30	-0.65	0.78	-0.53	-0.36
Dye 8		1.43	-1.03	>2.00		
	ΔGet^{T1}_{Iod} (eV)	ΔGet^{T1}_{EDB} (eV)	K^{sv}_{Iod} (M^{-1})	$\phi^{et(S1)}_{Iod}$	K^{sv}_{EDB} (M^{-1})	$\phi^{et(S1)}_{EDB}$
Dye 3	-0.27	0.36	303.6	0.928	88.6	0.913
Dye 6	-0.57	0.15	14.1	0.376	8.1	0.471
Dye 7	0.18	0.35	14.3	0.379	0.47	0.053
Dye 8	>1.27	0.6				

a: For Iod, the reduction potential of -0.7 V is used according to ref. [41].
b: calculated triplet state energy level at DFT level.

The singlet excited state energies (E_{S1}) of dyes were extracted by using the normalized UV-visible absorption and fluorescence spectra in acetonitrile (see Figure S5), and by using the crossing point of the two curves (See Table 3, 1.97 eV for dye 3; 2.00 eV for dye 6; 2.01 eV for dye 7). Conversely, no fluorescence spectrum could be recorded for dye 8 due to the presence of nitro group in this dye.

The oxidation potential (E_{ox}), the reduction potential (E_{red}) of for the electron transfer reaction of dyes 3, 6, 7, 8 have been extracted from their cyclic voltammograms (see Figure S6). The half peak oxidation potentials of dyes 3, 6, 7 (E_{ox}) were calculated and gathered in Table 3 (0.29 V for dye 3, 0.18 V for dye 6, 0.78 V for dye 7). However, there is no current observed in oxidation cycle of dye 8 (see Figure S6d), indicating that its oxidation potential could be greater than 2.00V. In contrast, the reduction potential of four dyes are located at -0.62 V, -0.60 V, -0.65 V, -1.03 V (for dye 3, 6, 7, 8, respectively) and showed in Table 3.

The free energy changes ΔG^{S1}_{Iod} or ΔG^{S1}_{EDB} for the electron transfer reaction between dyes and Iodonium salts or EDB were confirmed by equations (eq 3-6) and listed in Table 3 (ΔG_{Iod}= -0.98eV, ΔG_{EDB}= -0.35eV for dye 3; ΔG_{Iod}= -1.12eV, ΔG_{EDB}= -0.4eV for dye 6; ΔG_{Iod}= -0.53eV, ΔG_{EDB}= -0.36eV for dye 7). ΔG are < 0, which indicate the theoretical feasibility of these electron transfer reactions.

Calculations of the triplet energy levels E_{T1} (eV) of dyes 3, 6, 7, 8 were performed at DFT level, and gathered in Table 3. The triplet routes involved in mechanisms can be ruled out for the dye/EDB interactions due to all of their free energy changes at triplet state ΔGet^{T1} are greater than 0, even if the dye/Iod interactions are less than 0 except dye 7/Iod combination.

The photoinitiating ability of dyes was also studied by examining the fluorescence quenching experiments on dye 3, dye 6 and dye 7 in acetonitrile as well as their Stern-Volmer coefficients (Ksv) and the electron transfer quantum yields (ϕ_{et}) were also carried out (see Table 3). Linear fluorescence quenching processes were observed (see Figure 8a, c for dye 3, Figure S7a, c for dye 7) for all dye/Iod or dye/EDB

combinations except dye 8, fitting to the results of free energy changes discussed above. Their Stern-Volmer coefficients Ksv were determined by the slopes of Stern−Volmer treatment for fluorescence quenching (see Figure 8b, d for dye 3; Figure S7b, d for dye 7; Table 3) and high electron transfer quantum yields ϕ_{et} were calculated by equation (eq 2) (Table 3). These data are in full agreement with the mechanisms discussed in photolysis part 3.4.2, and 3.4.3.

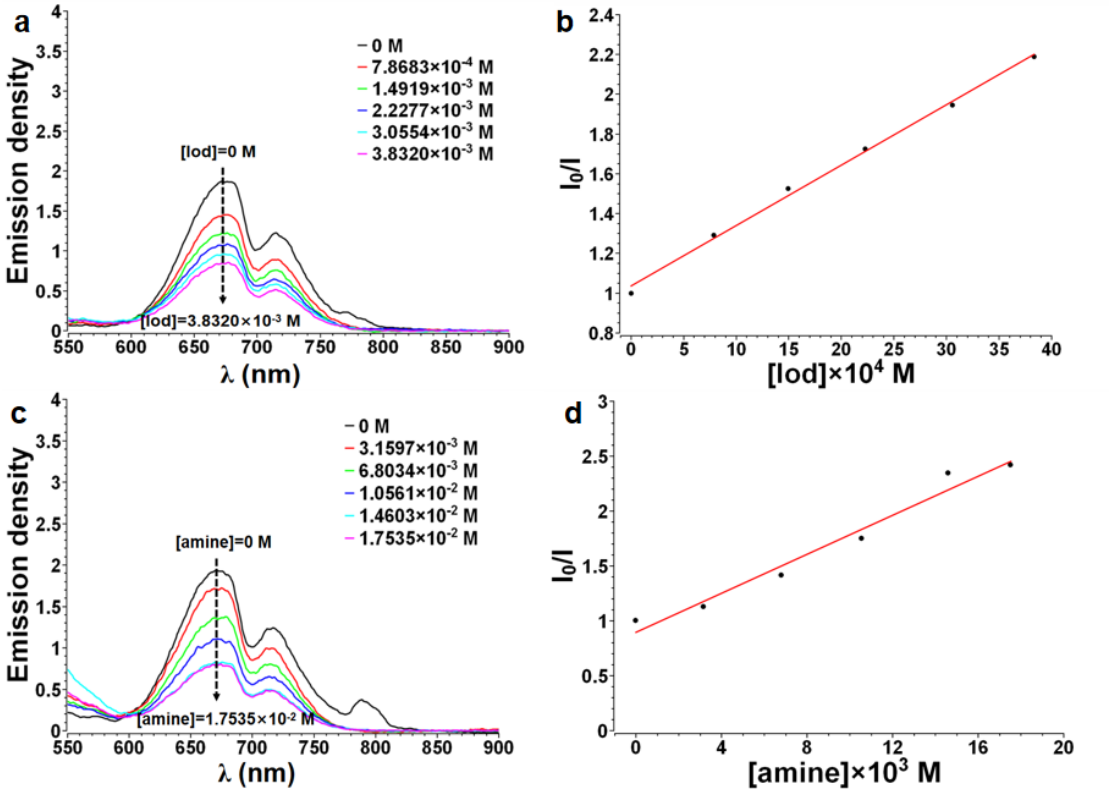

Figure 8. Fluorescence quenching of dye 3 (7.77×10^{-6}M in acetonitrile) by: **(a) iodonium salt (Iod); (c) amine (EDB).** Stern−Volmer treatment for fluorescence quenching of the **(b) dye 3/iodonium; (d) dye 3/EDB**.

3.4.5. ESR spin-trapping experiments

Confirmation of the proposed chemical mechanisms could be obtained by characterizing the $Ar^{\bullet}$ and $EDB^{\bullet}_{(-H)}$ radicals by ESR-spin trapping experiments. Selected dyes were separately mixed with Iod and EDB in *tert*-butylbenzene at the same

concentration ratio ([dye]=0.2mg/mL; [Iod]= 2mg/mL; [EDB]=2mg/mL) under nitrogen as a protection gas, then PBN (2mg/mL) used as the spin trap agent and dissolved into the solution.

For dye 8, the ESR spectra for dye 8/Iod and dye 8/EDB solutions characterized both before and after irradiation are given in Figure 9 as well as the spectra of dye 7/Iod and dye 7/EDB are presented in Figure S8. The same experiments were also done with the other two dyes (dye 3, 6), in the same conditions, and the results confirmed the formations of the expected radicals: PBN/Ar• was detected in the four dye/Iod solutions, while $PBN/EDB_{(-H)}$• was also detected for the four dye/EDB combinations. Particularly, dye 8/Iod and dye 8/EDB solutions were also characterized by ESR-spin experiment under irradiation of sunlight, and the spectra were showed in Figure 10, which indicates the radicals generated and chemical mechanisms occurred in photopolymerization of dye 8 under sunlight is same to LED. Interestingly, the sunlight-induced free radical polymerization initiated by dye 8-based PISs also can be performed in the mild weather conditions without sunlight: rainy, grey clouds. The ESR-spin experiments were carried out around 12:00 am on 3rd, Nov. 2020, in Mulhouse Area (+77° 43′ E, -47° 75′ N) of France, and the weather conditions were depicted in Figure S9.

Hyperfine Couplings Constants (HFC) for the PBN radical adducts are given in Table 4 by simulation of the curves of ESR spectra, and corresponding to the literature data.[57, 58] Thus, the feasibility of the chemical mechanisms presented above has clearly been proved.

Table 4. HFC constants determined by ESR-spin experiments for the four selected dyes.

	Dye 3	Dye 6	Dye 7	Dye 8 at 405nm LED	Dye 8 at sunlight
Iod	a_N=14.4 a_H=2.1	a_N=14.4 a_H=2.1	a_N=14.4 a_H=2.2	a_N=14.4 a_H=2.1	a_N=14.4 a_H=2.2

EDB	a_N=14.4 a_H=2.1	a_N=14.4 a_H=2.1	a_N=14.4 a_H=2.1	a_N=14.4 a_H=2.1	a_N=14.4 a_H=2.3

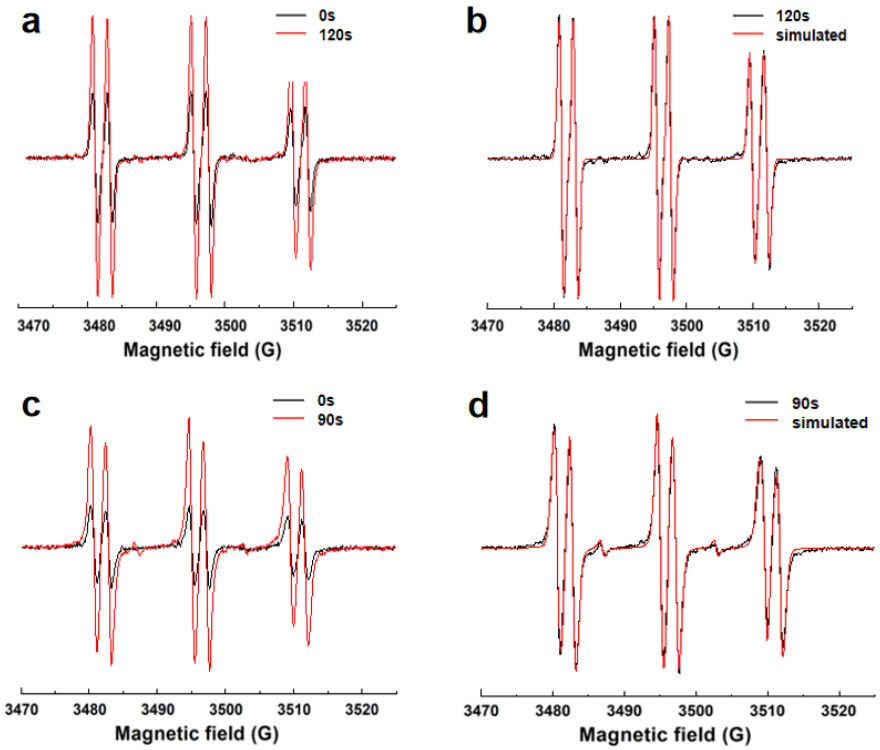

Figure 9. ESR spectra obtained from ESR-spin trapping experiments under **irradiation of 405nm LED** using PBN = 2 mg/mL (as the spin trap agent); Iod = 2 mg/mL, EDB = 2 mg/mL and dye 8= 0.2 mg/mL in *tert*-butylbenzene under N_2. **(a) dye 8/Iod PIS**, Irradiation time =120s (red) and =0s (black) spectra, respectively; **(b) dye 8/Iod PIS**, Irradiation time =120s experimental (black) and simulated (red) spectra; **(c) dye 8/EDB PIS,** Irradiation time =90s (red) and =0s (black) spectra; **(d) dye 8/EDB PIS,** Irradiation time =90s experimental (black) and simulated (red) spectra.

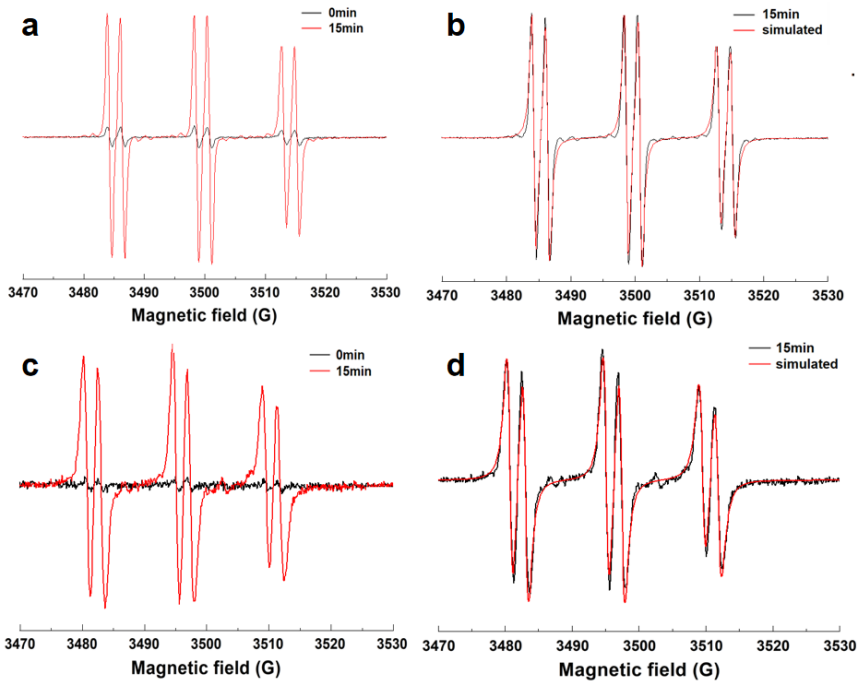

Figure 10. ESR spectra obtained from ESR-spin trapping experiments under **irradiation of sunlight** using PBN = 2 mg/mL (as the spin trap agent); Iod = 2 mg/mL, EDB = 2 mg/mL and dye 8= 0.2 mg/mL in *tert*-butylbenzene under N_2. (a) **dye 8/Iod PIS**, Irradiation time =15min (red) and =0min (black) spectra, respectively; **(b) dye 8/Iod PIS**, Irradiation time =15min experimental (black) and simulated (red) spectra; **(c) dye 8/EDB PIS,** Irradiation time =15min (red) and =0min (black) spectra; **(d) dye 8/EDB PIS,** Irradiation time =15min experimental (black) and simulated (red) spectra.

3.5. Direct laser write (DLW) experiments for the photocomposites with silica fillers.

To broaden the applications of the push-pull dyes, a possible application was proposed and examined by producing photocomposites by FRP. Photocomposites were prepared by adding silica fillers into the monomer (TA) at a weight ratio of 20%. PISs used in this part are the same as used before, namely, the dyes 3, 7 and 8/Iod/EDB three-component systems (0.1%/2%/2% in monomer, w/w/w). Here, the laser acts as the irradiation source to print the 3D patterns of photocomposites: “SEP”, “SRZ”, “021” (for dye 3, 7 and 8, respectively) with a high spatial resolution. The different 3D patterns

with high spatial resolution were characterized by profilometric observations as shown in Figure 11.

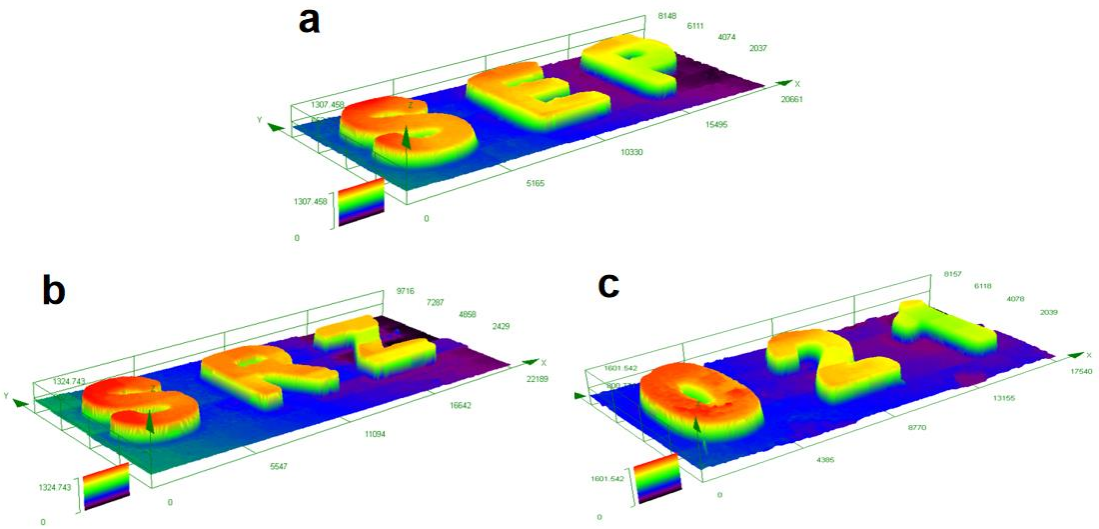

Figure 11. Free radical photopolymerization experiments in DLW experiments in TA. Characterization of 3D overall appearance of color patterns by numerical optical microscopy in the presence of: **(a)** dye 3/Iod/EDB/silica (0.1%/2%/2%/20% in TA, w/w/w); **(b)** dye 7/Iod/EDB/silica (0.1%/2%/2%/20% in TA, w/w/w/w); **(c)** dye 8/Iod/EDB/silica (0.1%/2%/2%/20% in TA, w/w/w/w).

4. Conclusion

In conclusion, 12 new push-pull dyes (never synthesized before) with a *N*-ethyl carbazole-1-allylidene group were synthesized and examined for their photoinitiation abilities and their applications in DLW experiments. To clarify the relevant photochemical mechanism, steady state photolysis and fluorescence experiments were carried out on the dye-based systems. In addition, the suggested chemical mechanisms were confirmed by ESR experiments. Interestingly, dye 8 proved to be the most reactive photoinitiator of the series upon irradiation with sunlight, indicating the advantages of dyes with push-pull structures for developing photoinitiators capable of efficiently initiating a polymerization process with sunlight. Moreover, polymer composites containing silica fillers could be successfully polymerized with several dyes examined

in this work. With aim at developing more green polymerization processes, future works will consist in developing water soluble dyes, paving the way towards the polymerization in emulsion.

Supplementary Materials: Figure S1. UV-vis absorption spectra of dyes 1-12; **Figure S2.** UV-vis absorption spectra of photolysis for dye 7; **Figure S3.** UV-vis absorption spectra of photolysis for dye 8; **Figure S4.** Consumption of dye 8 in photolysis process; **Figure S5.** Singlet state energy determination in acetonitrile for dye 3, 6 and 7; **Figure S6.** Cyclic voltammograms for dyes 3, 6, 7, 8; **Figure S7.** Fluorescence quenching of dye 7 by Iodonium salt and amine; **Figure S8.** ESR spectra of dye 7 obtained from ESR-spin trapping experiment. **Figure S9.** The Shortcuts of weather and address of experiments performed for sunlight irradiation.

Author Contributions: Conceptualization, JL, FD, PX.; methodology, JL, FD, PX, KS.; synthesis of dyes, FD and CP; software, BG.; validation, All authors; formal analysis, JL, FD, PX, KS; data curation, All authors; writing—original draft preparation, JL, FD, PX, KS; writing—review and editing, All authors.

Funding: China Scholarship Council (CSC) for Ke Sun. The Agence Nationale de la Recherche (ANR agency) is acknowledged for funding through the PhD grant of Corentin Pigot (ANR-17-CE08-0010 DUALITY project).

Acknowledgments: This research project is supported by China Scholarship Council (CSC) (No.201808440451). PX acknowledges funding from the “Australian Research Council (FT170100301)”. This work was granted access to the HPC resources of the Mesocentre of the University of Strasbourg.

Conflicts of Interest: The authors declare no conflict of interest.

References

（1）Wood, C. J.; Summers, G. H.; Gibson, E. A. Increased photocurrent in a tandem dye-sensitized solar cell by modifications in push–pull dye-design. *Chemical Communications* 2015, *51*(18), 3915-3918.

（2）Yella, A.; Mai, C. L.; Zakeeruddin, S. M.; Chang, S. N.; Hsieh, C. H.; Yeh, C. Y.; Grätzel, M. Molecular engineering of push–pull porphyrin dyes for highly efficient dye-sensitized solar cells: The role of benzene spacers. *Angewandte Chemie* 2014, *126*(11), 3017-3021.

（3）Cheema, H.; Baumann, A.; Loya, E. K.; Brogdon, P.; McNamara, L. E.; Carpenter, C. A.; Hammer, N. I.; Mathew, S; Risko, C.; Delcamp, J. H. Near-Infrared-Absorbing Indolizine-Porphyrin Push–Pull Dye for Dye-Sensitized Solar Cells. *ACS applied materials & interfaces* 2019, *11*(18), 16474-16489.

（4）Kivala, M.; Diederich, F. Acetylene-derived strong organic acceptors for planar and nonplanar push−pull chromophores. *Accounts of chemical research* 2019, *42*(2), 235-248.

（5）García, G.; Adamo, C.; Ciofini, I. Evaluating push–pull dye efficiency using TD-DFT and charge transfer indices. *Physical Chemistry Chemical Physics* 2013, *15*(46), 20210-20219.

（6）Cai, N.; Wang, Y.; Xu, M.; Fan, Y.; Li, R.; Zhang, M.; Wang, P. Engineering of Push-Pull Thiophene Dyes to Enhance Light Absorption and Modulate Charge Recombination in Mesoscopic Solar Cells. *Advanced Functional Materials* 2013, *23*(14), 1846-1854.

（7）Tehfe, M. A.; Dumur, F.; Graff, B.; Morlet-Savary, F.; Fouassier, J. P.; Gigmes, D.; Lalevée, J. New Push–Pull Dyes Derived from Michler's Ketone For Polymerization Reactions Upon Visible Lights. *Macromolecules* 2013, *46*(10), 3761-3770.

（8）Tehfe, M. A.; Dumur, F.; Graff, B.; Morlet-Savary, F.; Gigmes, D.; Fouassier, J. P.; Lalevée, J. Push–pull (thio) barbituric acid derivatives in dye photosensitized radical and cationic polymerization reactions under 457/473 nm laser beams or blue LEDs. *Polymer Chemistry* 2013, *4*(13), 3866-3875.

（9）Tehfe M. A.; Dumur, F.; Graff, B.; Morlet-Savary, F.; Gigmes, D.; Fouassier, J. P.; Lalevée, J. New push-pull dyes derived from Michler's ketone for polymerization reactions upon visible lights. *Macromolecules* 2013, *46*(10), 3761-3770.

（10）Xiao, P.; Frigoli, M.; Dumur, F.; Graff, B.; Gigmes, D.; Fouassier, J. P.; Lalevée, J. Julolidine or fluorenone based push-pull dyes for polymerization upon soft polychromatic visible light or green light. *Macromolecules* 2014, *47*(1), 106-112.

（11）Sun, K.; Pigot, C.; Chen, H.; Nechab, M.; Gigmes, D.; Morlet-Savary, F.; Graff, B.; Liu, S. Xiao, P.; Dumur, F.; Lalevée, J. Free radical photopolymerization and 3d printing using newly developed dyes: Indane-1, 3-dione and 1H-cyclopentanaphthalene-1, 3-dione derivatives as photoinitiators in three-component systems. *Catalysts* 2020, *10*(4), 463.

（12）Pigot, C.; Noirbent, G.; Peralta, S.; Duval, S.; Nechab, M.; Gigmes, D.; Dumur, F. Unprecedented Nucleophilic Attack of Piperidine on the Electron Acceptor during the Synthesis of Push-Pull Dyes by a Knoevenagel Reaction. *Helv. Chim. Acta* 2019, *102,* e1900229.

（13）Noirbent, G.; Dumur, F. Recent advances on nitrofluorene derivatives: Versatile electron acceptors to create dyes absorbing from the visible to the near and far-infrared region. *Materials* 2018, *11*(12), 2425.

（14）Blanchard-Desce, M.; Wortmann, R.; Lebus, S.; Lehn, J. M.; Krämer, P. Intramolecular charge transfer in elongated donor-acceptor conjugated polyenes. *Chem. Phys. Lett.* 1995, *243*(5–6), 526–532.

（15）Noirbent, G.; Pigot, C.; Bui, T.-T.; Péralta, S.; Nechab, M. ; Gigmes, D.; Dumur, F. Synthesis, optical and electrochemical properties of a series of push-pull dyes based on the 2-(3-cyano-4,5,5-trimethylfuran-2(5H)-ylidene) malononitrile (TCF) acceptor, *Dyes and Pigments* 2021, *184*, 108807.

（16）Paek, S.; Lee, J.K.; Ko, J. Synthesis and photovoltaic characteristics of push–pull organic semiconductors containing an electron-rich dithienosilole bridge for solution-processed small-molecule organic solar cells. *Sol. Energ. Mater. Solar Cells* 2014, *120*, 209–217.

（17）Xu, S. J.; Zhou, Z.; Liu, W.; Zhang, Z.; Liu, F.; Yan, H.; Zhu, X. A twisted thieno[3,4-*b*]thiophene-based electron acceptor featuring a 14-π-electron indenoindene core for high-performance organic photovoltaics. *Adv. Mater.* 2017, *29*(43), 1704510.

（18）Turkoglu, G.; Cinar, M.E.; Ozturk, T. Triarylborane-based materials for OLED applications. *Molecules* 2017, *22*(9), 1522.

（19）Karak, S.; Liu, F.; Russell, T.P.; Duzhko, V.V. Bulk charge carrier transport in push-pull type organic semiconductor. *ACS Appl. Mater. Interfaces* 2014, *6*(23), 20904–20912.

（20）Raimundo, J.M.; Blanchard, P.; Gallego-Planas, N.; Mercier, N.; Ledoux-Rak, I.; Hierle, R.; Roncali, J. Design and synthesis of push-pull chromophores for second-order nonlinear optics derived from rigidified thiophene-based π-conjugating spacers. *J. Org. Chem.* 2002, *67*(1), 205–218.

（21）El-Shishtawy, R. M.; Borbone, F.; Al-amshany, Z. M.; Tuzi, A.; Barsella, A.; Asiri, A. M.; Roviello, A. Thiazole azo dyes with lateral donor branch: Synthesis, structure and second order NLO properties. *Dyes and Pigments.* 2013, *96*(1), 45–51.

（22）Cesaretti, A.; Bonaccorso, C.; Elisei, F.; Fortuna, C. G.; Mencaroni, L.; Spalletti, A. Photoinduced Intramolecular Charge Transfer and Hyperpolarizability Coefficient in Push-Pull Pyridinium Salts with Increasing Strength of the Acceptor Group. *ChemPlusChem* 2018, *83*(11), 1021-1031.

（23）Motiei, H.; Jafari, A.; Naderali, R. Third-order nonlinear optical properties of organic azo dyes by using strength of nonlinearity parameter and Z-scan technique. *Optics & Laser Technology* 2017, *88*, 68-74.

（24）El-Shishtawy, R. M.; Al-Zahrani, F. A.; Afzal, S. M.; Razvi, M. A. N.; Al-amshany, Z. M.; Bakry, A. H.; Asiri, A. M. Synthesis, linear and nonlinear optical properties of a new dimethine cyanine dye derived from phenothiazine. *RSC advances* 2016, *6*(94), 91546-91556.

（25）Chaumel, F.; Jiang, H.; Kakkar, A. Sol−gel materials for second-order nonlinear optics. *Chemistry of materials* 2001, *13*(10), 3389-3395.

（26）Matsumoto S.; Kubodera K. I.; Kurihara T.; Kaino T. Nonlinear optical properties of an azo dye attached polymer. *Appl. Phys. Lett.* 1987, *51*(1), 1–2.

（27）Gao, S. H.; Xie, M. S.; Wang, H. X.; Niu, H. Y.; Qu, G. R.; Guo, H. M. Highly selective detection of Hg2+ ion by push–pull-type purine nucleoside-based flfluorescent sensor. *Tetrahedron* 2014, *70*(33), 4929– 4933.

（28）Allegrezza, M. L.; DeMartini, Z. M.; Kloster, A. J.; Digby, Z. A.; Konkolewicz, D. Visible and sunlight driven RAFT photopolymerization accelerated by amines: kinetics and mechanism. *Polymer Chemistry* 2016, *7*(43), 6626-6636.

（29）Wang, J.; Rivero, M.; Muñoz Bonilla, A.; Sanchez-Marcos, J.; Xue, W.; Chen, G.; Zhang, W; Zhu, X. Natural RAFT polymerization: recyclable-catalyst-aided, opened-to-Air, and sunlight-photolyzed RAFT polymerizations. *ACS Macro Letters* 2016, *5*(11), 1278-1282.

（30）Ciftci, M.; Tasdelen, M. A.; Yagci, Y. Sunlight induced atom transfer radical polymerization by using dimanganese decacarbonyl. *Polymer Chemistry* 2014, *5*(2), 600-606.

（31）Decker, C.; Bendaikha, T. Interpenetrating polymer networks. II. Sunlight-induced polymerization of multifunctional acrylates. *Journal of applied polymer science* 1998, *70*(11), 2269-2282.

（32）Fouassier, J. P.; Allonas, X.; Burget, D. Photopolymerization reactions under visible lights: principle, mechanisms and examples of applications. *Progress in organic coatings* 2003, *47*(1), 16-36.

（33）Tehfe, M. A.; Lalevee, J.; Gigmes, D.; Fouassier, J. P. Green chemistry: sunlight-induced cationic polymerization of renewable epoxy monomers under air. *Macromolecules* 2010, *43*(3), 1364-1370.

（34）Tehfe, M. A.; Lalevée, J.; Morlet-Savary, F.; Graff, B.; Fouassier, J. P. A breakthrough toward long wavelength cationic photopolymerization: Initiating systems based on violanthrone derivatives and silyl radicals. *Macromolecules* 2011, *44*(21), 8374-8379.

（35）Sun, K.; Liu, S.; Pigot, C.; Brunel, D.; Graff, B.; Nechab, M.; ... & Dumur, F. (2020). Novel Push–Pull Dyes Derived from 1H-cyclopenta [b] naphthalene-1, 3 (2H)-dione as Versatile Photoinitiators for Photopolymerization and Their Related Applications: 3D Printing and Fabrication of Photocomposites. *Catalysts, 10*(10), 1196.

（36）Dietlin, C.; Schweizer, S.; Xiao, P.; Zhang, J.; Morlet-savary, F.; Graff, B.; Fouassier, J. P.; Lalevée, J. Photopolymerization upon LEDs: new photoinitiating systems and strategies. *Polym. Chem.* 2015, *6*(21), 3895-3912.

（37）Lalevée, J.; Blanchard, N.; Tehfe, M.A.; Morlet-Savary, F.; Fouassier, J. P. Green bulb light source induced epoxy cationic polymerization under air using tris (2, 2′-bipyridine) ruthenium (II) and silyl radicals. *Macromolecules* 2010, *43*(24), 10191–10195.

（38）Lalevée, J.; Blanchard, N.; Tehfe, M.A.; Peter, M.; Morlet- Savary, F.; Gigmes, D.; Fouassier, J. P. Efficient dual radical/cationic photoinitiator under visible light: a new concept. *Polym. Chem.,* 2011, *2*(9), 1986–1991.

（39）Xu, Y. Y.; Ding, Z. F.; Liu, F. Y.; Sun, K.; Dietlin, C.; Lalevée, J.; Xiao, P. 3D Printing of Polydiacetylene Photocomposite Materials: Two Wavelengths for Two Orthogonal Chemistries. *ACS Applied Materials & Interfaces* 2019, *12*(1), 1658-1664.

（40）Rehm, D.; Weller, A. Kinetics of fluorescence quenching by electron and H-atom transfer. *Isr. J. Chem.* 1970, *8*(2), 259–271.

（41）Romanczyk, P. P.; Kurek, S. S. The Reduction Potential of Diphenyliodonium Polymerisation Photoinitiator Is Not −0.2 V vs. SCE. A Computational Study *Electrochim. Acta* 2017, *225*, 482–485.

（42）Fouassier, J. P.; Lalevée, J. Photoinitiators for polymer synthesis – scope, reactivity, and efficiency. Weinheim: *John Wiley & Sons*, 2012.

（43）Zhang, J.; Dumur, F.; Xiao, P.; Graff, B.; Bardelang, D.; Gigmes, D.; Fouassier, J. P.; Lalevée, J. Structure design of naphthalimide derivatives: Toward versatile photoinitiators for near-UV/visible LEDs, 3D printing, and water-soluble photoinitiating systems. *Macromolecules* 2015, *48*(7), 2054–2063.

（44）Xiao, P.; Dumur, F.; Zhang, J.; Fouassier, J.-P.; Gigmes, D.; Lalevée, J. Copper complexes in radical photoinitiating systems: applications to free radical and cationic polymerization upon visible LEDs. *Macromolecules* 2014, *47*(12), 3837–3844.

（45）James, B.; Frisch, A. Exploring chemistry with electronic structure methods. *Gaussian, Incorporated*, 1996.

（46）Frisch, M. J.; Trucks, G. W.; Schlegel, H. B.; Scuseria, G. E.; Robb, M. A.; Cheeseman, J. R.; Zakrzewski, V. G.; Montgomery, J. A.; Stratmann, R. E.; Burant, J. C.; Dapprich, S.; Millam, J. M.; Daniels, A. D.; Kudin, K. N.; Strain, M. C.; Farkas, O.; Tomasi, J.; Barone, V.; Cossi, M.; Cammi, R.; Mennucci, B.; Pomelli, C.; Adamo, C.; Clifford, S. J.; Ochterski, W.; Petersson, G. A.; Ayala, P. Y.; Cui, Q.; Morokuma, K.; Salvador, P.; Dannenberg, J. J.; Malick, D. K.; Rabuck, A. D.; Raghavachari, K.; Foresman, J. B.; Cioslowski, J.; Ortiz, J. V.; Baboul, A. G.; Stefanov, B. B.; Liu, G.; Liashenko, A.; Piskorz, P.; Komaromi, I.; Gomperts, R.; Martin, R. L.; Fox, D. J.; Keith, T.; Al-Laham, M. A.; Peng, C. Y.; Nanayakkara, A.; Challacombe, M.; Gill, P. M. W.; Johnson, B.; Chen, W.; Wong, M. W.; Andres, J. L.; Gonzalez, C.; Head-Gordon, M.; Replogle, E. S.; Pople, J. *A. Gaussian 03, Revision B-2, Gaussian Inc., Pittsburgh, PA*, 2003.

（47）Dumur, F.; Mayer, C. R.; Dumas, E.; Miomandre, F.; Frigoli, M.; Sécheresse, F. New chelating stilbazonium-like dyes from Michler's ketone. *Organic letters*, 2008, *10*(2), 321-324.

（48）Pigot, C.; Noirbent, G.; Peralta, S.; Duval, S.; Bui, T.-T.; Aubert, P.-H.; Nechab, M.; Gigmes, D.; Dumur, F. New push-pull dyes based on 2-(3-oxo-2,3-dihydro-1H-cyclopenta[b]naphthalen-1-ylidene)malononitrile: An amine-directed synthesis, *Dyes and Pigments*, 2020, *175*, 108182.

（49）Landmesser, T.; Linden, A.; Hansen, H.-J.; A novel route to 1-substituted 3-(dialkylamino)-9-oxo-9H-indeno[2,1-c]-pyridine-4-carbonitriles. *Helv. Chim. Acta* 2008, *91*(2), 265-284.

（50）Helmy, S.; Oh, S.; Leibfarth, F.A.; Hawker, C.J.; Read de Alaniz, J. Design and synthesis of donor-acceptor Stenhouse adducts: a visible light photoswitch derived from furfural. *J. Org. Chem.* 2014, *79*(23), 11316-11329.

（51）Gao, M.; Su, H.; Lin, Y.; Ling, X.; Li, S.; Qin, A.; Zhong Tang, B. Photoactivatable aggregation-induced emission probes for lipid droplets-specific live cell imaging, *Chem. Sci.* 2017, *8*(3),1763-1768.

（52）Cao, C.; Zhou, X.; Xue, M.; Han, C.; Feng, W.; Li, F. Dual near-infrared-emissive luminescent nanoprobes forratiometric luminescent monitoring of clo−in living organisms. *ACS Appl. Mater. Interfaces.* 2019, *11*(17), 15298-15305.

（53）Cui, Y.; Ren, H.; Yu, J.; Wang, Z.; Qian, G. An indanone-based alkoxysilane dye with second order nonlinear optical properties. *Dyes and Pigments*, 2009, *81*(9), 53-57.

（54）Batsanov, A. S.; Bryce, M. R.; Davies, S. R.; Howard, J. A. K.; Whitehead, R.; Tanner, B.K. Studies on π-acceptor molecules containing the dicyanomethylene group. X-ray crystal structure of the charge-transfer complex of tetramethyltetrathiafulvalene

and 2,3-dicyano-1,4-naphthoquinone: $(TMTTF)_3$-$(DCNQ)_2$, *J. Chem. Soc., Perkin Trans. 2: Phys. Org. Chem.* 1993, 3, 313-319.

（55）Perepichka, D.F.; Perepichka, I.F.; Ivasenko, O.; Moore, A.J.; Bryce, M.R.; Kuzmina, L.G.; Batsanov, A.S.; Sokolov, N.I.; Combining high electron affinity and intramolecular charge transfer in 1,3-dithiole–nitrofluorene push–pull diads, *Chem. Eur. J.* 2008, *14*(9), 2757-2770.

（56）Pigot, C.; Noirbent, G.; Bui, T.-T.; Péralta, S.; Gigmes, D.; Nechab, M.; Dumur, F. Push-pull chromophores based on the naphthalene scaffold: Potential candidates for optoelectronic applications, *Materials* 2019, *12*(8), 1342.

（57）Haire, L.D.; Krygsman, P.H.; Janzen, E.G.; Oehler, U.M. Correlation of radical structure with EPR spin adduct parameters: utility of the proton, carbon-13, and nitrogen-14 hyperfine splitting constants of aminoxyl adducts of PBN-nitronyl-^{13}C for three-parameter scatter plots. *J. Org. Chem.* 1988, *53,* 4535-4542.

（58）Ohto, N.; Niki, E.; Kamiya, Y. Study of autoxidation by spin trapping. Spin trapping of peroxyl radicals by phenyl N-t-butyl nitrone. *J. Chem. Soc., Perkin Trans. 2*, 1977**,** *13*, 1770-1774.